

MINERALOGIA, 39, No. 1–2: 41–52 (2008)

DOI: 10.2478/v10002-008-0003-7

www.Mineralogia.pl

MINERALOGICAL SOCIETY OF POLAND

POLSKIE TOWARZYSTWO MINERALOGICZNE



Original paper

Thermochemical characterization of $\text{Ca}_4\text{La}_6(\text{SiO}_4)_6(\text{OH})_2$ a synthetic La- and OH-analogous of britholite: implication for monazite and LREE apatites stability

Emilie JANOTS^{1,2} *, Fabrice BRUNET³, Bruno GOFFÉ³, Christophe POINSSOT⁴,
Michael BURCHARD⁵ and Lado CEMIC⁶

¹ Institut für Geologie, University of Bern, Switzerland; e-mail: emiliejants@uni-muenster.de

² Institut für Mineralogie, WWU Münster, Germany

³ Laboratoire de Géologie, CNRS UMR8538, Paris, France

⁴ DEN/DPC/SECR, CEA, Saclay, France

⁵ Mineralogisches Institut, Universität-Heidelberg, Germany

⁶ Institut für Geowissenschaften, Universität Kiel, Germany

* Corresponding author

Received: December 22, 2007

Accepted: April 03, 2008

Abstract. In this contribution, monazite (LREEPO_4) solubility is addressed in a chemical system involving REE-bearing hydroxylapatite, $(\text{Ca,LREE})_{10}(\text{PO}_4)_6(\text{SiO}_4)_6(\text{OH})_2$. For this purpose, a synthetic (La)- and (OH)-analogous of britholite, $\text{Ca}_4\text{La}_6(\text{SiO}_4)_6(\text{OH})_2$, was synthesised and its thermodynamic properties were measured. Formation enthalpy of $-14,618.4 \pm 31.0 \text{ kJ}\cdot\text{mol}^{-1}$ was obtained by high-temperature drop-solution calorimetry using a Tian-calvet twin calorimeter (Bochum, Germany) at 975 K using lead borate as solvent. Heat capacities (C_p) were measured in the 143–323 K and 341–623 K ranges with an automated Perkin-Elmer DSC 7. For calculations of solubility diagrams at 298 K, the GEMS program was used because it takes into account solid solutions. In conditions representative of those expected in nuclear waste disposal, calculations show that La-monazite is stable from pH = 4 to 9 with a minimum of solubility at pH = 7. La-bearing hydroxylapatite precipitates at pH > 7 with a nearly constant composition of 99% hydroxylapatite and 1% La-britholite. Each mineral buffers solution at extremely low lanthanum concentrations ($\log\{\text{La}\} = 10^{-10}$ – $10^{-15} \text{ mol}\cdot\text{kg}^{-1}$ for pH = 4 to 13). In terms of chemical durability, both La-monazite and La-rich apatite present low solubility, a requisite property for nuclear-waste forms.

Key-words: monazite, britholite, apatite, calorimetry, nuclear waste form

1. Introduction

Its ubiquity, high chemical durability and resistance to metamictisation confer to monazite qualities of a robust U-Th-Pb chronometer (e.g. Spear, Pyle 2002) as well as a potential candidate as nuclear waste form (Boatner 1988; Ewing, Wang 2002). In order to predict its long term behavior, thermodynamic properties of monazite have been recently (re)-examined. Experimental solubility product data have been obtained for synthetic end-members of monazite-(La), -(Nd) and -(Sm) (Rai et al. 2003; Poitrasson et al. 2004; Cetiner et al. 2005). Formation enthalpies and entropies have been measured by high temperature drop-solution (Ushakov et al. 2001; Ushakov et al. 2004) and low-temperature adiabatic calorimetry (Thiriet et al. 2005), respectively. Heat capacities of monazite have been measured in the temperature range of 450 to 1570 K by drop calorimetry (Popa et al. 2006; Popa et al. 2007). A thermochemical study compiling measured formation enthalpy, entropy and heat capacity was also given for synthetic monazite-(La) (Janots et al. 2007). With those thermochemical properties, solubility of monazite end-members and corresponding REE speciation can be nowadays calculated for different conditions of temperature (T), pressure (P), pH and aqueous speciation. At monazite equilibrium, REE concentrations can also be estimated, but predicted concentrations could be limited by a potential control of a less soluble phase than monazite. In such case, less soluble phases may replace monazite. Of particular interest is hydroxylapatite because it is the major phosphate repository, it can incorporate LREE under sedimentary and diagenetic conditions (e.g. Lev et al. 1998) and it is also proposed as nuclear waste form (Weber 1981; Carpena, Lacout 1997). Furthermore, replacement of monazite by REE-rich apatite at very high metamorphic conditions has already been described in granulites. Amongst the available thermodynamic properties of REE-bearing apatite, formation enthalpies of oxyapatite (Risbud et al. 2001; Ardhaoui et al. 2006b) and fluorobriholite (Ardhaoui et al. 2006a) have already been measured.

In the present study, thermochemical data have been measured and calculations attempted to investigate the conditions under which REE-bearing apatite is less soluble than monazite and controlled the REE concentrations in solution. For this purpose, calorimetric data have been collected on a synthetic (La)- and (OH)- equivalent of britholite, $\text{Ca}_4\text{La}_6(\text{SiO}_4)_6(\text{OH})_2$, which forms a solid solution with the apatite, $\text{Ca}_{10}(\text{PO}_4)_6(\text{OH},\text{F})_2$ (Ito 1968). Formation enthalpy and heat capacity (C_p) function have been derived from high-temperature solution calorimetry and differential scanning calorimetry, respectively. Solubility diagrams were calculated for geochemical conditions representative of high level deposit in clay.

2. Methods

Britholite equivalent, $\text{Ca}_4\text{La}_6(\text{SiO}_4)_6(\text{OH})_2$, has been synthesised from stoichiometric tetraethylorthosilicate-based gels that were calcinated at 1073 K (ambient pressure). Resulting gels have been held at 873 K and 150 MPa for 30 days in a cold-seal vessel. Product was characterised by X Ray diffraction, with a Siemens D5000 diffractometer (Kiel University, Germany). All peaks in the diffraction pattern can be attributed to the britholite structure (Fig. 1). Lattice parameters were obtained by rietveld refinement with a symmetry respecting the $P6_3/m$ space

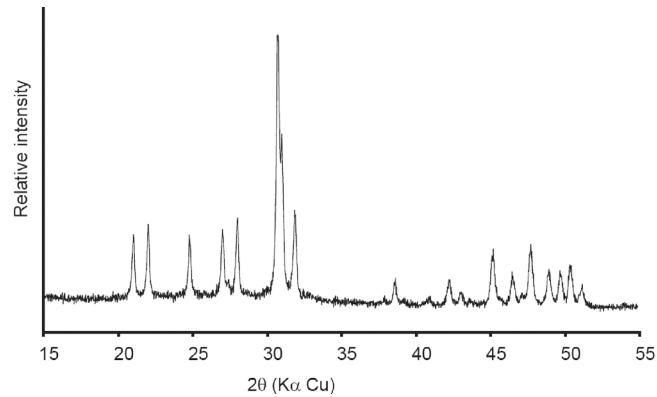


Fig. 1. XRD diffraction pattern of synthetic La-hydroxybritholite

(Oberti et al. 2001). Data retrieved for the synthetic $\text{Ca}_4\text{La}_6(\text{SiO}_4)_6(\text{OH})_2$ (Table 1) compares well with the unit cell parameters of the britholite-(Ce) obtained by Noe et al. (1993). As expected from ionic radius of La and Y, $\text{Ca}_4\text{La}_6(\text{SiO}_4)_6(\text{OH})_2$ shows a larger volume than the britholite-(Y). Homogeneity, composition and grain size of the synthetic products were analysed using scanning electron microscopy (Hitachi S-2500 with EDS detector), Raman microspectroscopy (Renishaw spectrometer, $\lambda = 532 \text{ nm}$, ENS-Paris, France) and electron microprobe analysis (SX-50, Jussieu, France).

Formation enthalpies were derived from high-temperature drop-solution calorimetry (Navrotsky 1997) in the Tian-Calvet twin calorimeter described by (Kahl, Maresch 2001) and located at the Institut for Geology, Mineralogy and Geophysics (Ruhr University, Bochum, Germany). Sample pellets of 5 to 8 mg are dropped from room temperature (290–293 K) into a lead-borate solvent ($2\text{PbO} \cdot \text{B}_2\text{O}_3$) held at the calorimeter temperature (975 K). Measurements are performed under dynamic conditions (Navrotsky et al. 1994), i.e. under an argon stream (flow rate of $1.5 \text{ cm}^3 \cdot \text{s}^{-1}$), because volatile-bearing phases are investigated (e.g. carbonates and hydroxides). Before each set of measurements (typically, five measurements on both calorimeter sides), platinum scraps (30 mg) are dropped into the solvent in order to determine the calorimeter calibration factor. Because samples are equilibrated, before being dropped, at a temperature between 290 and 293 K instead of 298.15 K (reference temperature), measured drop-solution enthalpy values (ΔH_{ds}) are corrected using the C_p function of the sample. These C_p are either taken from literature (CaCO_3 , SiO_2 and CaSiO_3 in Robie and Hemingway 1995) in or were measured by DSC (britholite, LaOH_3). In order to achieve the reaction cycles required to retrieve

TABLE I

Lattice parameters of synthetic $\text{Ca}_4\text{La}_6(\text{SiO}_4)_6(\text{OH})_2$, natural britholite-(Ce) and britholite-(Y)

Phase	a	b	c	γ	$V(\text{\AA}^3)$
$\text{Ca}_4\text{La}_6(\text{SiO}_4)_6(\text{OH})_2$	9.67	9.66	7.12	120.02	575.8 (6)
Britholite-(Ce)	9.63		7.03		564.60
Britholite-(Y)	9.43		6.81		524.45

formation enthalpy data, additional sample powders were used for drop-solution measurements: CaCO₃ (Aesar, 99.99%). Gem-quality specimens (from the mineral collection of the Ruhr-University, Bochum, Germany) of Brazilian quartz (99.9% purity) and wollastonite, Ca_{2.98–3.00}Si_{3.00–3.03}O₃, from Kropfmuhl (Germany) were used.

Heat capacities were measured in the 143–323 K and 341–623 K ranges with an automated Perkin-Elmer DSC 7 (Institute of Geosciences, Kiel University, Germany). Temperature calibration, purge gas and other technical details are found in Bosenick et al. (1996) and Bertoldi et al. (2001) for the measurements in the high-temperature and low-temperature regions, respectively. Measurements are performed on 20 mg of sample placed in a gold pan (6 mm diameter) and covered with a thin gold lid. A heat-capacity datum is obtained by measuring alternatively, a blank (empty pan), a standard for calibration (pan loaded with corundum) and the sample of interest (pan with sample). Heat capacities were collected in step-scanning mode as described in Bosenick et al. (1996), with a heating rate of 10 K·min⁻¹. The Cp-calibration factor is obtained from synthetic corundum measurements, using the Cp-function by Ditmars and Douglas (1971). Correction for Au-pan weight differences is calculated using the gold Cp polynomial by Robie et al. (1979).

3. Thermochemical data

Drop-solution enthalpies (ΔH_{ds}) for britholite and its reactant phases were measured in lead borate solvent at 975 K (Table 2). The reaction cycle used to derive britholite formation enthalpy $\Delta H_{f,298}^{\circ}$ is given as an example in Table 3. Volatile components (H₂O and CO₂) are assumed to be totally released by the lead borate melt (Navrotsky et al. 1994) and flushed by the argon stream (*i.e.* under dynamic conditions). The dissolution enthalpy of CaCO₃ (Table 2) is consistent with published data obtained under dynamic conditions (Navrotsky et al. 1994;

TABLE 2

Corrected drop-solution enthalpies (ΔH_{ds}) from this study compared to data from literature

Sample	ΔH_{ds} measured (kJ·mol ⁻¹)	ΔH_{ds} literature (kJ·mol ⁻¹)
Britholite OH, Ca ₄ La ₆ (SiO ₄) ₆ (OH) ₂	1024.0 ± 16.4 (12)	
La(OH) ₃	170.1 ± 3.8 (11)	
Calcite, CaCO ₃	190.9 ± 0.8 (17)	191.1 ± 1.1 (7) ^(a) ; 194.1 ± 0.9 ^(b) ; 193.4 ± 0.7 (10) ^(c) ; 189.6 ± 1.1 (9) ^(d)
Quartz, SiO ₂	38.8 ± 1.1 (8)	38.8 ± 0.8 (9) ^(a) ; 38.4 ± 0.8 ^(b) ; 39.1 ± 0.3 (9) ^(c) ; 40.0 ± 0.2 (6) ^(e)
Wollastonite, CaSiO ₃	105.8 ± 3.1 (8)	105.4 ± 0.7 (8) ^(e)

ΔH_{ds} from (a) Kahl, Maresch (2001) (b) Grevel et al. (2001) (c) Kisevela et al. (1996) (d) Navrotsky (1994) (e) Chai, Navrotsky (1993).

Numbers in parentheses are the number of measurements of drop-solution values.

Reported uncertainties are two standard deviation of the mean.

TABLE 3

Thermochemical cycle used to derive the standard enthalpy of formation from the elements $\Delta H_{f,el}^{(298)}$ of britholite, $\text{Ca}_4\text{La}_6(\text{SiO}_4)_6(\text{OH})_2$

Reaction		ΔH (kJ·mol ⁻¹)
$\text{Ca}_2\text{La}_3(\text{SiO}_4)_3(\text{OH})_{(298)} \rightarrow \text{Ca}_2\text{La}_3(\text{SiO}_4)_3(\text{OH})_{(975)}$	(1) ΔH_{ds} $\text{Ca}_4\text{La}_6(\text{SiO}_4)_6(\text{OH})_2$	1024.0 ± 16.4
$\text{CO}_2_{(298)} \rightarrow \text{CO}_2_{(975)}$	(2) $\Delta H_{[298-975]}\text{CO}_2$	32.2
$\text{CaCO}_3_{(298)} \rightarrow \text{CaCO}_3_{(975)}$	(3) $\Delta H_{ds} \text{CaCO}_3$	190.9 ± 0.8
$\text{La}(\text{OH})_3_{(298)} \rightarrow \text{La}(\text{OH})_3_{(975)}$	(4) $\Delta H_{ds} \text{La}(\text{OH})_3$	170.1 ± 3.8
$\text{SiO}_2_{(298)} \rightarrow \text{SiO}_2_{(975)}$	(5) $\Delta H_{ds} \text{SiO}_2$	38.8 ± 1.1
$\text{H}_2\text{O}_{(298)} \rightarrow \text{H}_2\text{O}_{(975)}$	(6) $\Delta H_{[298-975]}\text{H}_2\text{O}$	25.1
$4\text{CaCO}_3_{(298)} + 6\text{La}(\text{OH})_3_{(298)} + 6\text{SiO}_2_{(298)} \rightarrow$ $\rightarrow \text{Ca}_4\text{La}_6(\text{SiO}_4)_6(\text{OH})_2_{(298)} + 4\text{CO}_2_{(298)} + 8\text{H}_2\text{O}_{(298)}$	(7) $\Delta H_{ox,298}^{\circ}$ $\text{Ca}_4\text{La}_6(\text{SiO}_4)_6(\text{OH})_2$	
$\Delta H(7) = -2\Delta H(1) - 4\Delta H(2) - 8\Delta H(6) + 4\Delta H(3) + 6\Delta H(4) + 6\Delta H(5)$		
$\text{C}_{(298)} + \frac{1}{2}\text{O}_2_{(298)} \rightarrow \text{CO}_2_{(298)}$	(8) $\Delta H_f^{\circ} \text{CO}_2^{(a)}$	-393.5 ± 0.1
$\text{Ca}_{(298)} + \text{C}_{(298)} + \frac{3}{2}\text{O}_2_{(298)} \rightarrow \text{CaCO}_3_{(298)}$	(9) $\Delta H_f^{\circ} \text{CaCO}_3^{(a)}$	-1207.4 ± 1.3
$\text{La}_{(298)} + \frac{3}{2}\text{O}_2_{(298)} + \frac{3}{2}\text{H}_2_{(298)} \rightarrow \text{La}(\text{OH})_3_{(298)}$	(10) $\Delta H_f^{\circ} \text{La}(\text{OH})_3^{(b)}$	-1416.1 ± 1.0
$\text{Si}_{(298)} + \text{O}_2_{(298)} \rightarrow \text{SiO}_2_{(298)}$	(11) $\Delta H_f^{\circ} \text{SiO}_2^{(a)}$	-910.7 ± 1.0
$\text{H}_2_{(298)} + \frac{1}{2}\text{O}_2_{(298)} \rightarrow \text{H}_2\text{O}_{(298)}$	(12) $\Delta H_f^{\circ} \text{H}_2\text{O}^{(a)}$	-241.8 ± 0.0
$4\text{Ca}_{(298)} + 6\text{La}_{(298)} + 6\text{Si}_{(298)} + \text{H}_2_{(298)} + 13\text{O}_2_{(298)} \rightarrow$ $\rightarrow \text{Ca}_4\text{La}_6(\text{SiO}_4)_6(\text{OH})_2_{(298)}$	(13) ΔH_f° $\text{Ca}_4\text{La}_6(\text{SiO}_4)_6(\text{OH})_2$	$-14,618.4 \pm 31.0$
$\Delta H(13) = \Delta H(7) - 4\Delta H(8) - 8\Delta H(12) + 4\Delta H(9) +$ $+ 6\Delta H(10) + 6\Delta H(11)$		

Data from (a) Robie et al. (1995) (b) Diakonov et al. (1998).

Kahl, Maresch 2001). The reaction cycle presented for britholite (Table 3) involves CaCO_3 and yields a formation enthalpy of $-14,618.4 \pm 31.0$ kJ·mol⁻¹. A second cycle built up with CaSiO_3 instead of CaCO_3 yields $\Delta H_{f,298}^{\circ} = -14,626.2 \pm 32.2$ kJ·mol⁻¹ for britholite. The close agreement between the formation enthalpy derived from these two reaction cycles validates the assumption of CO_2 degassing from the solvent. For the thermochemical calculations, we used arbitrarily data derived from cycle with calcite. In comparison to data published for REE-bearing apatite, the value determined in this study compares with formation enthalpy of La-oxyapatite $\text{La}_{9.33}(\text{SiO}_4)_6\text{O}_2$ ($-14,611$ kJ·mol⁻¹) obtained by drop solution calorimetry in lead borate solvent (Risbud et al. 2001). Astonishingly, our value is comprised between those of the Nd-fluorobritholite, $\text{Ca}_4\text{Nd}_6(\text{SiO}_4)_6\text{F}_2$, ($-12,162$ kJ·mol⁻¹) and the La-oxyapatite, $\text{Ca}_4\text{La}_6(\text{SiO}_4)_6\text{O}$, ($-16,904$ kJ·mol⁻¹) both measured by microcalorimetry in acid solutions (Ardhaoui et al. 2006a, 2006b).

Heat-capacity data for britholite could not be measured above 623 K due to decomposition (dehydration) in the vicinity of that temperature. Mean C_p values from three to five DSC

TABLE 4

Cp data of La-hydroxybritholite $\text{Ca}_4\text{La}_6(\text{SiO}_4)_6(\text{OH})_2$ obtained by DSC

T [K]	C_p	2σ	T [K]	C_p	2σ
143.15	477	26	321.15	875	61
146.15	485	25	343.15	851	21
149.15	495	25	348.15	860	22
152.15	501	29	353.15	868	21
155.15	505	31	358.15	874	21
158.15	513	27	363.15	879	20
161.15	521	28	368.15	883	19
164.15	526	30	373.15	886	19
167.15	535	26	378.15	889	19
170.15	544	27	383.15	893	19
173.15	549	29	388.15	896	18
176.15	556	24	393.15	900	18
179.15	569	23	398.15	904	17
182.15	575	25	403.15	909	16
185.15	581	21	408.15	913	15
188.15	593	20	413.15	919	14
191.15	601	21	418.15	926	14
194.15	607	20	423.15	933	17
197.15	620	17	443.15	916	17
200.15	629	20	448.15	918	18
203.15	636	19	453.15	922	18
206.15	648	16	458.15	924	19
209.15	658	21	463.15	928	19
212.15	668	21	468.15	930	20
215.15	677	20	473.15	935	20
218.15	688	23	478.15	939	20
221.15	697	26	483.15	942	19
243.15	747	33	488.15	947	19
246.15	750	32	493.15	953	18
249.15	755	30	498.15	958	18
252.15	761	33	503.15	964	16
255.15	767	33	508.15	971	16
258.15	775	33	513.15	977	14
261.15	786	32	518.15	985	13
264.15	801	32	523.15	992	15
267.15	796	30	543.15	975	20
270.15	783	33	548.15	978	21
273.15	786	34	553.15	980	18
276.15	793	33	558.15	982	19
279.15	800	34	563.15	988	21
282.15	804	37	568.15	989	17
285.15	807	36	573.15	993	16
288.15	811	39	578.15	997	15
291.15	815	42	583.15	1 002	14
294.15	825	40	588.15	1 006	13
297.15	832	42	593.15	1 011	10
300.15	833	44	598.15	1 016	9
303.15	841	45	603.15	1 021	8
306.15	848	51	608.15	1 026	7
309.15	847	53	613.15	1 032	8
312.15	859	53	618.15	1 038	9
315.15	863	55	623.15	1 044	12
318.15	863	57			

temperature scans, are listed with their two standard deviation of the mean in Table 4. The precision for low-temperature and superambient DSC data is around 2–7% and 1–3%, respectively (Fig. 2). Heat capacities measured with DSC shows difference below 5% with those derived from an oxide summation method (Berman, Brown 1985). The heat-capacity function of britholite measured by DSC was fitted to the Cp-polynomial proposed by Maier and Kelley (1932) in order to be input in the database related to the Gibbs Energy Minimization Selector program (GEMS, developed at the PSI, Villigen, Switzerland).

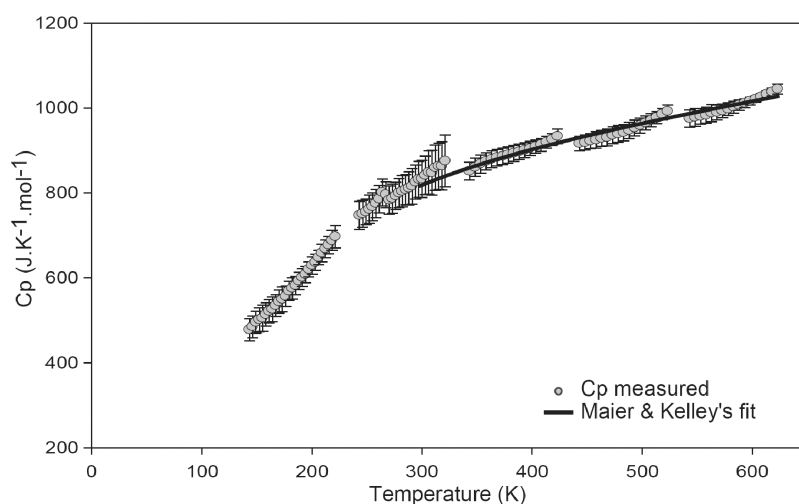


Fig. 2. DSC data obtained on britholite-(La) fit to Berman and Brown's polynomial (1985)

Since low-temperature Cp data have not been measured for britholite, its entropy was approximated with the oxide summation method proposed by Holland (1989). This summation method includes a molar volume correction ($S-V$) to the entropy and can predict entropy within a few percents when the coordination of the oxide components is taken into account. In order to derive britholite entropy, ($S-V$) values are taken from Holland (1989), apart from ($S-V$) La_2O_3 which was estimated in Janots et al. (2007). Taking a britholite molar volume of $351.2 \text{ cm}^3 \cdot \text{mol}^{-1}$, the predicted entropy of britholite is found to be equal to $868.6 \text{ J} \cdot \text{mol}^{-1} \text{ K}^{-1}$.

4. Thermochemical calculations – discussion

The strategy developed here has been to compare monazite solubility in multicomponent chemical systems with or without considering the britholite-apatite solid solution.

Solubility diagrams were calculated with the GEMS code to compare the respective chemical solubility of monazite and apatite-britholite solid solutions under conditions of high-level waste storage. The GEMS program computes equilibrium phase assemblage and speciation in a complex chemical system from its total bulk composition by Gibbs free energy minimisation. GEMS was used in this study because it can account for solid solutions. Calculations were performed at ambient conditions with the database related to the SUPCRT92 code enriched with

thermochemical data derived in this study or relevant phases taken from the literature: LaPO_4 (Janots et al. 2007), $\text{La}(\text{OH})_3$ (Diakonov et al. 1998), $\text{La}_2(\text{CO}_3)_3 \cdot 8\text{H}_2\text{O}$ (Nguyen et al. 1993), $\text{La}(\text{OH})_{0.8}(\text{CO}_3)_{1.1} \cdot 0.1\text{H}_2\text{O}$ (Gämsjäger et al. 1995) and the hydroxylapatite (Robie et al. 1995). Solid solutions between the hydroxylapatite and britholite were considered as ideal. We selected conditions modeled from the interactions between an alkaline plume and bentonite (Gaucher et al. 2004), which are supposed to approach those of a solution in a nuclear deposit with concrete and a clay barrier. Bulk composition corresponds to the following elemental concentrations: $0.014 \text{ mol} \cdot \text{kg}^{-1}$ of Ca, $3.43 \cdot 10^{-4} \text{ mol} \cdot \text{kg}^{-1}$ of Si and $2.46 \cdot 10^{-3} \text{ mol} \cdot \text{kg}^{-1}$ of C. Relative solubility of monazite compared to apatite-britholite solid solution as well as lanthanum speciation are here addressed as a function of pH.

First, solubility diagram of monazite at 298 K was established in the $\text{La}_2\text{O}_3\text{-P}_2\text{O}_5\text{-H}_2\text{O-CO}_2$ system considering 0.01 mole of monazite in one kilogram of water with 0.00246 mole of CO_2 . Using GEMS program, lanthanum aqueous species and saturating La-phases have been calculated from pH = 3 to 13. pH variations were computed from an inverse titration by adding HNO_3 and NaOH . Figure 3 presents lanthanum speciation and the La-phases at equilibrium. It shows that monazite is oversaturated throughout the entire range of pH and buffers the solution at concentrations of lanthanum below $10^{-9} \text{ mol} \cdot \text{L}^{-1}$ from pH = 5.5 to pH = 10. The minimum solubility is found at pH around 8.5. Apart from monazite, $\text{La}(\text{OH})_3$ controls lanthanum concentration only at pH above 11. It is noteworthy that lanthanum nitrate complex formation due to HNO_3 titration influence negligibly the lanthanum concentrations at pH > 5.

Monazite solubility at 298 K was also investigated in the $\text{La}_2\text{O}_3\text{-CaO-P}_2\text{O}_5\text{-SiO}_2\text{-H}_2\text{O-CO}_2$ system to address monazite stability in a chemical system comprising the britholite-hydro-

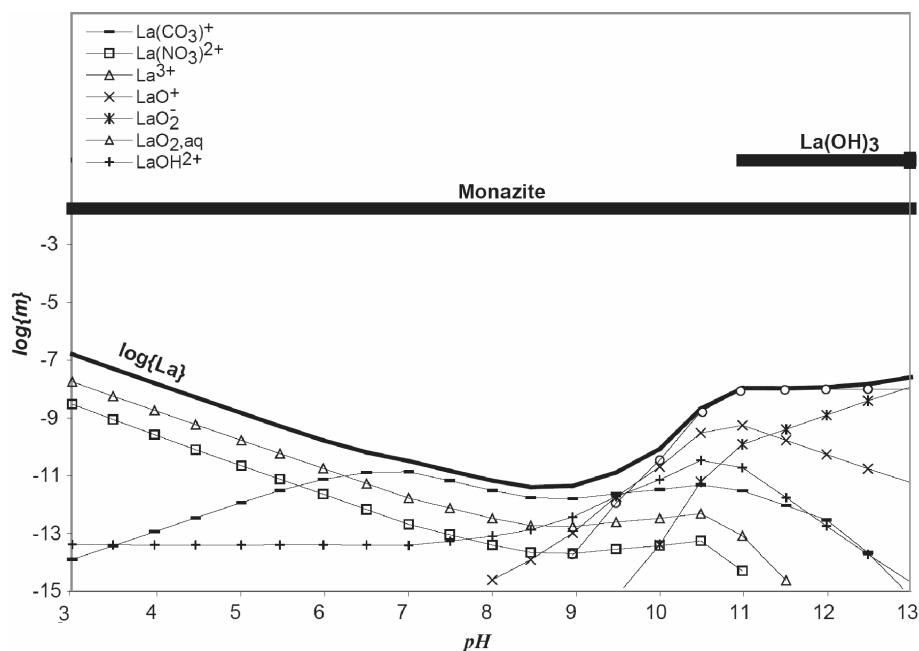


Fig. 3. Solubility-Speciation diagram in the $\text{La}_2\text{O}_3\text{-P}_2\text{O}_5\text{-H}_2\text{O-CO}_2$ system for 0.01 mole of monazite in one kilogram H_2O with 0.00246 mole of CO_2 at pH = 3–13

xylapatite solid solution. Rather than considering an amount of monazite, concentrations of lanthanum and phosphorus were fixed to be representative of concentrations encountered in nature. Phosphorus concentration ($1.10^{-7} \text{ mol}\cdot\text{kg}^{-1}$) corresponds to the concentrations at equilibrium with the hydroxylapatite at neutral pH. The lanthanum concentration ($1.10^{-9} \text{ mol}\cdot\text{kg}^{-1}$) is based on lanthanide concentrations measured in water in the area of the fossil reactor of Oklo (Gabon). This latter concentration is of the same order as those derived from our thermochemical data (Fig. 3) for $\text{pH} = 5\text{--}10$. Figure 4 shows that monazite is stable from $\text{pH} = 4$ to 9 with a minimum of solubility at $\text{pH} = 7$. The solid solution between apatite and britholite precipitates at $\text{pH} > 7$ with a nearly constant composition of 99% hydroxylapatite and 1% britholite. In its respective stability field, each mineral has a very low solubility and buffers the solution at comparable low lanthanum concentrations ($\log\{\text{La}\} = 10^{-10}\text{--}10^{-15} \text{ mol}\cdot\text{kg}^{-1}$ for $\text{pH} = 4$ to 13).

This thermochemical diagram shows some consistencies with natural observations. Calculated apatite composition, with 99% hydroxylapatite and 1% La-britholite, is compatible with the REE concentrations in apatite, formed in sedimentary and diagenetic conditions. REE-bearing apatite has been often described in diagenetic rocks and REE contents $\sim 0.3\%$ were measured by Lev et al. (1998). By comparison, the britholite end-member is only found in high-temperature rocks, such as magmatic or granulite-facies rocks (e.g. Arden, Halden 1999). In our calculations at 298 K, monazite is more stable than REE-apatite on acid to neutral pH. This can explain why monazite occurs in replacement of apatite during granite weathering and soil formation (Banfield, Eggleton 1989; Taunton et al. 2000). Even under high temperature

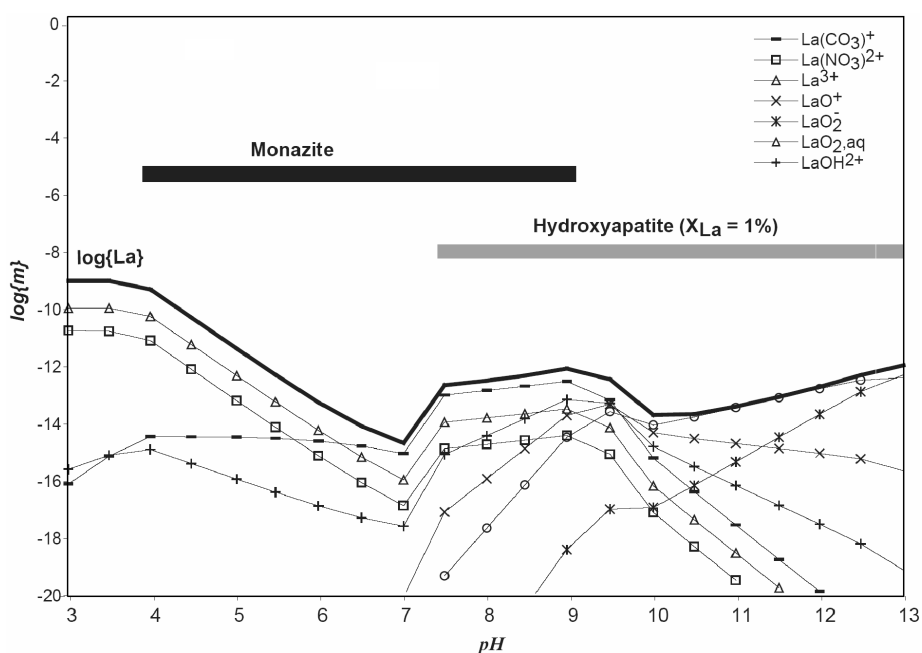


Fig. 4. Solubility-Speciation diagram in the $\text{La}_2\text{O}_3\text{-P}_2\text{O}_5\text{-CaO-SiO}_2\text{-H}_2\text{O-CO}_2$ system obtained with GEMS code at $\text{pH} = 3\text{--}13$. Concentrations are derived from Gaucher et al. (2004) apart for phosphorus and lanthanum concentrations fixed at $10^{-7} \text{ mol}\cdot\text{kg}^{-1}$ and $10^{-9} \text{ mol}\cdot\text{kg}^{-1}$, respectively (explanations and discussion in text)

conditions, the apatite replacement by monazite appear as a recurrent feature (e.g. Harlov et al. 2002; Harlov et al. 2007). In contrast, replacement of monazite by apatite has been rarely described and when documented it reveals that REE will be incorporated by secondary REE-phases such as allanite rather than apatite (Finger et al. 1998).

Furthermore, calculated concentrations at equilibrium ($\{La\} = 10^{-10}$ – 10^{-15} mol·kg⁻¹ for pH = 4 to 13) are consistent with concentrations measured experimentally during the dissolution of Nd-britholite, Ca₉Nd(PO₄)₅SiO₄F₂ ($\{Nd\} < 10^{-12}$ mol·kg⁻¹ at pH = 7, Chairat et al. 2006). In this experimental study, Nd release rates were slower than Ca, P and Si at neutral pH due to the precipitation of a secondary phosphate phase. These last observations are coherent with our calculations where monazite appears more stable than apatite under acidic to neutral conditions.

The solid solution composition close to the hydroxylapatite end-member is more stable thermochemically than the silicated britholite end-member, under the conditions of our model. In terms of chemical durability at 298 K, it is expected thermodynamically that britholite will react to form hydroxylapatite and/or monazite in the presence of phosphate aqueous species. Both monazite and La-bearing hydroxylapatite show remarkable low solubility around neutral pH that limits lanthanum concentrations in solution. Hence, it confers to them good chemical qualities as potential matrix for nuclear waste-form. While hydroxides or carbonates of lanthanum are the stable solid phases in the La₂O₃-H₂O-CO₂ system (Diakonov et al. 1998), they are no longer stable in the La₂O₃-CaO-SiO₂-H₂O-CO₂ system. The absence of these synthetic La-phases in complex chemical system tends to show that La-phases with natural occurrences are more stable than synthetic ones, as shown already experimentally for Th-phases (Goffé et al. 2002). During diagenesis, REE are redistributed often with the involvement of REE-enriched phosphate phases such as apatite, monazite but also florencite (review in Bock et al. 2004). In fact, florencite is observed in weathered granite (e.g. Banfield, Eggleton 1989), marine sediment (e.g. Rasmussen 1996), hydrothermal rock (Gaboreau et al. 2005) as well as pelite (Janots et al. 2006). Hence, prediction of REE distribution at sedimentary conditions will require further solubility studies in more complex system including REE-bearing phases, such as florencite (Gaboreau, Vieillard 2004).

Acknowledgements. This research project was financially supported by the Swiss National fond (No 20020-101826/1 and 200021-103479), the NOMADE (CEA-CNRS) and French-German PROCOPE programs. The paper has been greatly improved by the critical and constructive comments of two anonymous reviewers.

5. References

- ARDEN K., HALDEN N., 1999: Crystallisation and alteration history of britholite in-rare-earth-element-enriched pegmatitic segregations associated with the Eden lake complex. *The Canadian Mineralogist* 37, 1239–1253.
- ARDHAOU K., COULET M.V., BEN CHERIFA A., CARPENA J., ROGEZ J., JEMAL M., 2006a: Standard enthalpy of formation of neodymium fluorbritholites. *Thermochimica Acta* 444(2), 190–194.
- ARDHAOU K., ROGEZ J., BEN CHERIFA A., JEMAL M., SATRE P., 2006b: Standard enthalpy of formation of lanthanum oxybritholites. *Journal of Thermal Analysis and Calorimetry* 86(2), 553–559.
- BANFIELD J.F., EGGLETON R.A., 1989: Apatite replacement and rare-earth mobilization, fractionation, and fixation during weathering. *Clays and Clay Minerals* 37(2), 113–127.
- BERMAN R.G., BROWN T.H., 1985: A Thermodynamic model for multicomponent melts, with application to the system CaO-Al₂O₃-SiO₂ – reply. *Geochimica et Cosmochimica Acta* 49(2), 613–614.

- BERTOLDI C., BENISEK A., CEMIC L., DACHS E., 2001: The heat capacity of two natural chlorite group minerals derived from differential scanning calorimetry. *Physics and Chemistry of Minerals* 28(5), 332–336.
- BOATNER L.A., SALES B.C., 1988: Monazite, Amsterdam.
- BOCK B., HUROWITZ J. A., McLENNAN S.M., HANSON G.N., 2004: Scale and timing of rare earth element redistribution in the Taconian foreland of New England. *Sedimentology* 51(4), 885–897.
- BOSENICK A., GEIGER C.A., CEMIC L., 1996: Heat capacity measurements of synthetic pyrope-grossular garnets between 320 and 1000 K by differential scanning calorimetry. *Geochimica et Cosmochimica Acta* 60(17), 3215–3227.
- CARPENA J., LACOUT J.L., 1997: Des apatites naturelles aux apatites synthétiques- Utilisation des apatites comme matrice de conditionnement de déchets nucléaires séparés. *Actualité Chimique* 2, 3–9.
- CETINER Z.S., WOOD S.A., GAMMONS C.H., 2005: The aqueous geochemistry of the rare earth elements. Part XIV. The solubility of rare earth element phosphates from 23 to 150 degrees C. *Chemical Geology* 217(1–2), 147–169.
- CHAIRAT C., OELKERS E.H., SCHOTT J., LARTIGUE J.E., 2006: An experimental study of the dissolution rates of Nd-britholite, an apatite-structured actinide-bearing waste storage host analogue. *Journal of Nuclear Materials* 354(1–3), 14–27.
- DIAKONOV II, TAGIROV B.R., RAGNARSDOTTIR K.V., 1998: Standard thermodynamic properties and heat capacity equations for rare earth element hydroxides. I. La(OH)₃(s) and Nd(OH)₃(s). Comparison of thermochemical and solubility data. *Radiochimica Acta* 81(2), 107–116.
- DITMARS D.A., DOUGLAS T.B., 1971: Measurement of relative enthalpy of pure alpha-Al₂O₃ (Nbs heat capacity and enthalpy standard reference material no 720) From 273 to 1173 K. *Journal of Research of the National Bureau of Standards Section a-Physics and Chemistry A* 75(5), 401–420.
- EWING R.C., WANG L.M., 2002: Phosphates as nuclear waste forms. In: *Phosphates: Geochemical, Geobiological, and Materials Importance Reviews in Mineralogy & Geochemistry*, pp. 673–699.
- FINGER F., BROSKA I., ROBERTS M.P., SCHERMAIER A., 1998: Replacement of primary monazite by apatite-allanite-peidote coronas in an amphibolite facies granite gneiss from the eastern alps. *American Mineralogist* 83, 248–58.
- GABOREAU S., BEAUFORT D., VIEILLARD P., PATRIER P., BRUNETON P., 2005: Aluminum phosphate-sulfate minerals associated with proterozoic unconformity-type uranium deposits in the east alligator river uranium field, northern territories, Australia. *Canadian Mineralogist* 43, 813–827.
- GABOREAU S., VIEILLARD P., 2004: Prediction of Gibbs free energies of formation of minerals of the alunite supergroup. *Geochimica et Cosmochimica Acta* 68(16), 3307–3316.
- GÄMSJÄGER H., MARHOLD H., KONIGSBERGER E., TSAI Y.J., KOLMER H., 1995: Solid-Solute Phase-Equilibria in Aqueous-Solutions .9. Thermodynamic Analysis of Solubility Measurements – La(OH)_m(CO₃)_qrH₂O. *Zeitschrift Fur Naturforschung Section a Journal of Physical Sciences* 50(1), 59–64.
- GAUCHER E.C., BLANC P., MATRAY J.M., MICHAU N., 2004: Modeling diffusion of an alkaline plume in a clay barrier. *Applied Geochemistry* 19(10), 1505–1515.
- GOFFÉ B., JANOTS E., BRUNET F., POINSSOT C., 2002: Breakdown of thorium phosphate-diphosphate (TPD), Th₄(PO₄)₄P₂O₇, at 320 degrees C, 50 MPa in Ca-bearing systems, or why TPD does not occur in nature. *Comptes Rendus Geoscience* 334(14), 1047–1052.
- HARLOV D.E., ANDERSSON U.B., FORSTER H.J., NYSTROM J.O., DULSKI P., BROMAN C., 2002: Apatite-monzite relations in the kiirunavaara magnetite-apatite ore, northern sweden. *Chemical Geology* 191, 47–72.
- HARLOV D.E., MARSCHALL H.R., HANEL M., 2007: Fluorapatite-monzite relationships in granulite-facies metapelites, Schwarzwald, southwest Germany. *Mineralogical magazine*, 71(2), 223–234.
- HOLLAND T.J.B., 1989: Dependence of Entropy On Volume For Silicate and Oxide Minerals – a Review and a Predictive Model. *American Mineralogist* 74(1–2), 5–13.
- ITO J., 1968: Silicate Apatites and oxyapatites. *American Mineralogist* 53(5–6), 890–907.
- JANOTS E., BRUNET F., GOFFÉ B., POINSSOT C., BURCHARD M., CEMIC L., 2007: Thermochemistry of monazite-(La) and dissakisite-(La): Implications for monazite and allanite stability in metapelites. *Contributions to Mineralogy and Petrology* 154(1), 1–14.
- JANOTS E., NEGRO F., BRUNET F., GOFFÉ B., ENGI M., BOUYBAOUENE M.L., 2006: Evolution of the REE mineralogy in HP-LT metapelites of the Sebti complex, Rif, Morocco: Monazite stability and geochronology. *Lithos* 87(3–4), 214–234.

- KAHL W.A., MARESCH W.V., 2001: Enthalpies of formation of tremolite and talc by high-temperature solution calorimetry – a consistent picture. *American Mineralogist* 86(11–12), 1345–1357.
- LEV S.M., McLENNAN S.M., MEYERS W.J., HANSON G.N., 1998: A petrographic approach for evaluating trace-element mobility in a black shale. *Journal of Sedimentary Research* 68(5), 970–980.
- MAIER C.G., KELLEY K.K., 1932: An equation for the representation of high temperature heat content data. *American Chemical Society Journal* 54, 3243–3246.
- NAVROTSKY A., 1997: Progress and new directions in high temperature calorimetry revisited. *Physics and Chemistry of Minerals* 24(3), 222–241.
- NAVROTSKY A., RAPP R.P., SMELIK E., BURNLEY P., CIRCONI S., CHAI L., BOSE K., 1994: The behavior of H₂O and CO₂ in high-temperature lead borate solution calorimetry of volatile-bearing phases. *American Mineralogist* 79(11–12), 1099–1109.
- NGUYEN A.M., KONIGSBERGER E., MARHOLD H., GAMSJAGER H., 1993: Solid-solute phase-equilibria in aqueous-solutions. 8. The standard gibbs energy of La₂(CO₃)₃·8H₂O. *Monatshefte für Chemie* 124(10), 1011–1018.
- NOE D.C., HUGHES J.M., MARIANO A.N., DREXLER J.W., KATO A., 1993: The crystal structure of monoclinic britholite-(Ce) and britholite-(Y). *Zeitschrift für Kristallographie* 206, 233–246.
- OBERTI R., OTTOLINI L., DELLA VENTURA G., PARODI G.C., 2001: On the symmetry and crystal chemistry of britholite: New structural and microanalytical data. *American Mineralogist* 86(9), 1066–1075.
- POITRASSON F., OELKERS E., SCHOTT J., MONTEL J.M., 2004: Experimental determination of synthetic NdPO₄ monazite end-member solubility in water from 21 degrees C to 300 degrees C: Implications for rare earth element mobility in crustal fluids. *Geochimica et Cosmochimica Acta* 68(10), 2207–2221.
- POPA K., KONINGS R.J.M., GEISLER T., 2007: High-temperature calorimetry of (La_(1-x)Ln_(x))PO₄ solid solutions. *Journal of Chemical Thermodynamics* 39(2), 236–239.
- POPA K., SEDMIDUBSKY D., BENES O., THIRIET C., KONINGS R.J.M., 2006: The high-temperature heat capacity of LnPO₄ (Ln = La, Ce, Gd) by drop calorimetry. *Journal of Chemical Thermodynamics* 38(7), 825–829.
- RAI D., FELMY A.R., YUI M., 2003: Thermodynamic model for the solubility of NdPO₄(c) in the aqueous Na⁺-H⁺-H₂PO₄⁻-HPO₄²⁻-OH⁻-Cl⁻-H₂O system. *Journal of Radioanalytical and Nuclear Chemistry* 256(1), 37–43.
- RASMUSSEN B., 1996: Early-diagenetic REE-phosphate minerals (florencite, gorceixite, crandallite, and xenotime) in marine sandstones: A major sink for oceanic phosphorus. *American Journal of Science* 296(6), 601–632.
- RISBUD A.S., HELEAN K.B., WILDING M.C., LU P., NAVROTSKY A., 2001: Enthalpies of formation of lanthanide oxyapatite phases. *Journal of Materials Research* 16(10), 2780–2783.
- ROBIE R.A., HEMINGWAY B.S., 1995: Thermodynamic properties of minerals and related substances at 298.15 K and 1 bar (105 Pascals) pressure and at higher temperatures. Government Printing Office, Washington, 461p.
- ROBIE R.A., HEMINGWAY B.S., FISHER J.R., 1979: Thermodynamic properties of minerals and related substances at 298.15 K and 1 Bar (105 Pascals) pressure and at higher temperatures. U.S. Government Printing Office, Washington, 454 p.
- SPEAR F.S., PYLE J.M., 2002: Apatite, monazite, and xenotime in metamorphic rocks. In: *Phosphates: Geochemical, Geobiological, and Materials Importance Reviews in Mineralogy & Geochemistry*, pp. 293–335.
- TAUNTON A.E., WELCH S.A., BANFIELD J.F., 2000: Microbial controls on phosphate and lanthanide distributions during granite weathering and soil formation. *Chemical Geology* 169, 371–82.
- THIRIET C., KONINGS R.J.M., JAVORSKY P., MAGNANI N., WASTIN F., 2005: The low temperature heat capacity of LaPO₄ and GdPO₄, the thermodynamic functions of the monazite-type LnPO₄ series. *Journal of Chemical Thermodynamics* 37(2), 131.
- USHAKOV S.V., HELEAN K.B., NAVROTSKY A., BOATNER L.A., 2001: Thermochemistry of rare-earth orthophosphates. *Journal of Materials Research* 16(9), 2623–2633.
- USHAKOV S.V., NAVROTSKY A., FARMER J.M., BOATNER L.A., 2004: Thermochemistry of the alkali rare-earth double phosphates, A₃RE(PO₄)₂. *Journal of Materials Research* 19(7), 2165–2175.
- WEBER W.J., 1981: Radiation-damage in a rare-earth apatite structure. *American Ceramic Society Bulletin* 60(9), 934–934.